

NO reduction with ethanol on $\text{MoO}_3/\text{Al}_2\text{O}_3$ and $\text{CeO}_2\text{-ZrO}_2$ -supported Pd catalysts

Leonardo F. de Mello, Maria Auxiliadora S. Baldanza,
Fábio B. Noronha¹, M. Schmal*

*NUCAT-PEQ-COPPE, Universidade Federal do Rio de Janeiro, Ilha do Fundão,
COPPE, C.P. 68502, CEP 21941, Rio de Janeiro, Brazil*

Abstract

The reduction of NO with ethanol on $\text{MoO}_3/\text{Al}_2\text{O}_3$ and $\text{CeO}_2\text{-ZrO}_2$ -supported Pd catalysts was studied. The Pd/ $\text{CeO}_2\text{-ZrO}_2$ sample showed higher activity for the conversion of NO and higher selectivity for N_2 formation when compared to the Pd- $\text{MoO}_3/\text{Al}_2\text{O}_3$ sample. The CO chemisorption results showed that the CeZr mixed oxide chemisorbed a higher amount of CO, and this is related to a higher reducibility capacity of this compound when compared to MoO_3 . Furthermore, TPD analysis of adsorbed NO and ethanol showed that the Pd/ $\text{CeO}_2\text{-ZrO}_2$ catalyst has a higher ability of dissociating NO to N_2 and of decomposition of ethanol with the formation of CO_2 . Also, TPSR experiments showed that on Pd-8Mo/ Al_2O_3 , ethanol competes with NO for adsorption sites on partially reduced molybdenum oxide. This was not the case for the Pd/ $\text{Ce}_{0.75}\text{Zr}_{0.25}\text{O}_2$ catalyst, where both NO and ethanol adsorb and decompose on the partially reduced mixed oxide surface. These facts are probably related to the better performance of this catalyst in relation to the Pd- $\text{MoO}_3/\text{Al}_2\text{O}_3$ catalyst for the NO + ethanol reaction.

© 2003 Elsevier B.V. All rights reserved.

Keywords: NO reduction; Ethanol; Pd catalyst

1. Introduction

The first generation of automotive catalytic converters were made only to oxidize CO and hydrocarbons (HC). The catalysts were a combination of Pt and Pd supported on high surface area $\gamma\text{-Al}_2\text{O}_3$, stabilized with La_2O_3 [1].

The growing need to control NO_x emissions led to the addition of Rh to the Pt or Pd catalysts. This technology, known as three-way catalysis (TWC), in-

involved the simultaneous oxidation of CO and HC and the reduction of NO_x in a narrow, close to stoichiometric, air/fuel ratio [1]. This meant that the catalyst worked in slightly reducing and also oxidizing conditions. In order to keep the air to fuel ratio as close as possible to the stoichiometric value, cerium oxide was added to these catalysts. Due to its redox properties, CeO_2 works as an oxygen-storing component, releasing it during reducing conditions and absorbing it during oxidizing conditions [2]. Thus, the three-way catalysts consisted on the noble metals Pt and Rh (5:1 ratio), high surface area cerium oxide (10–20 wt.%) and $\gamma\text{-Al}_2\text{O}_3$.

The main disadvantage of CeO_2 is the loss of its oxygen storage capacity (OSC) due to particle sinterization at the high operating temperatures found in

* Corresponding author. Fax: +55-21-2906626.

E-mail addresses: fabiobel@int.gov.br (F.B. Noronha), schmal@peq.coppe.ufrj.br (M. Schmal).

¹ Present address: Laboratório de Catálise, Instituto Nacional de Tecnologia, Rio de Janeiro, Brazil.

vehicles, leading to the deactivation of the catalyst. The incorporation of ZrO_2 in the crystalline structure of CeO_2 , with the formation of a CeO_2 - ZrO_2 solid solution, increased not only the thermal stability, but also the oxygen storage capacity [3]. Normally, the addition of growing amounts of ZrO_2 lowers the temperature for reduction of Ce^{4+} . However, the optimum amount of zirconium oxide regarding the thermal stability and OSC value depends on the preparation method [4]. Hori et al. [5] observed that the optimum Zr concentration was around 25% (molar) for the $\text{Ce}_x\text{Zr}_{1-x}\text{O}_2$ samples prepared by co-precipitation of hydroxides.

Recently, the development of vehicles that operate with a narrow air/fuel ratio together with more stable supports are leading to the use of Pd-only catalysts, which allows to work at higher temperatures.

Although there are works showing the promoting effect of the $\text{Ce}_x\text{Zr}_{1-x}\text{O}_2$ support on the oxidation of CO and NO reduction by CO [6,7], no information of the role of this support on the reduction of NO by ethanol is found in the literature. This is an important issue in Brazil, where the fuel used in vehicles has a high amount of ethanol (22%) in gasoline.

Pd-Mo catalysts were used in Brazil on catalytic converters for ethanol fueled vehicles. Recent works showed that the addition of MoO_3 to $\text{Pd}/\text{Al}_2\text{O}_3$ promoted the dissociation of NO to N_2 during the NO + CO reaction [8,9]. This effect was explained through a redox mechanism where NO adsorbs and dissociates on the partially reduced molybdenum oxide and the oxygen from the NO molecule is used for the oxidation of CO on the Pd sites. These catalysts were also tested for the reduction of NO with ethanol. In this case, a promoting effect of the addition of MoO_3 to the $\text{Pd}/\text{Al}_2\text{O}_3$ catalyst was not observed.

The objective of this work is to study the performance of $\text{Pd}/\text{Ce}_{0.75}\text{Zr}_{0.25}\text{O}_2$ catalyst for the reduction of NO with ethanol and compare with the Pd-Mo catalysts.

2. Experimental

2.1. Catalysts preparation

The $\text{Ce}_{0.75}\text{Zr}_{0.25}\text{O}_2$ support was prepared by the co-precipitation of the corresponding salts, using a 2 M aqueous solution of $(\text{NH}_4)_2\text{Ce}(\text{NO}_3)_6$ (Aldrich)

and a solution of $\text{ZrO}(\text{NO}_3)_2$ (Aldrich), in the presence of excess NH_4OH (Merck) at room temperature [5]. Following this, the precipitate was washed until the eluting water showed a neutral pH. The material was calcined at 773 K for 1 h. The addition of molybdenum to alumina was carried out by wet impregnation with an aqueous solution of ammonium heptamolybdate containing 8 wt.% Mo ($8\text{Mo}/\text{Al}_2\text{O}_3$). Pd was added using a solution of $\text{Pd}(\text{NO}_3)_2$ (Merck) by dry impregnation ($\text{Pd}/\text{Ce}_{0.75}\text{Zr}_{0.25}\text{O}_2$) and wet impregnation ($\text{Pd}-8\text{Mo}/\text{Al}_2\text{O}_3$). The catalysts were then dried at 373 K for 24 h, calcined under flowing air (50 ml/min) at 773 K for 1 h, at a heating rate of 5 K/min. The amount of Pd used in both catalysts was 1% (w/w).

2.2. Catalyst characterization

The specific area (BET) measurements were made by N_2 adsorption at an ASAP-2000 (Micromeritics) equipment. X-ray diffraction (DRX) analyses to verify the formation of the CeZr mixed oxide were carried out on a Miniflex, Rigaku equipment, using $\text{Cu K}\alpha$ radiation.

The H_2 and CO chemisorption measurements were made on an ASAP-2000C (Micromeritics) equipment. Prior to reduction, the catalysts were dried at 423 K for 30 min. The samples were then reduced under pure hydrogen ($30\text{ cm}^3/\text{min}$) at 773 K (5 K/min) and vacuum was made at the reduction temperature for 1 h followed by cooling to the adsorption temperature. The irreversible adsorption was determined at 343 K for hydrogen and 298 K for carbon monoxide according to the method described by Benson et al. [10].

The temperature programmed desorption (TPD) analyses were carried out on a system coupled to a quadrupole mass spectrometer (Balzers, PRISMA). After drying under He flow at 823 K for 30 min, the catalysts were reduced under pure hydrogen at 773 K for 1 h. Either NO or ethanol adsorption was made at room temperature with a continuous flow of NO/He (1% NO in He-AGA) or ethanol/He mixtures. The ethanol/He mixture was obtained by passing helium through a saturator containing ethanol at room temperature. After adsorption, TPD measurements were carried out by heating the samples with a 20 K/min rate up to 823 K, under He flow. The products were continuously monitored by the Quadstar mass spectrometer

program (Balzers, PRISMA) as described before [9].

The temperature programmed surface reaction (TPSR) was performed in the same apparatus as the TPD analysis. The sample was purged with helium ($50 \text{ cm}^3/\text{min}$) from room temperature up to 823 K ($10 \text{ K}/\text{min}$), cooled to room temperature and reduced under flowing H_2 ($30 \text{ cm}^3/\text{min}$) up to 773 K ($5 \text{ K}/\text{min}$), remaining at that temperature for 1 h. Ethanol was adsorbed at room temperature until saturation of the surface. After adsorption, the sample was purged with He and a flow of a 1% NO/He mixture ($50 \text{ cm}^3/\text{min}$) was passed as the temperature was raised at $20 \text{ K}/\text{min}$ until 823 K.

2.3. Catalytic tests

The NO + ethanol reaction tests were made in a glass microreactor coupled to a gas chromatograph equipped with a chromosorb 102 column and cryogen. Prior to the reaction, the catalysts were pre-treated with He at 823 K for 30 min, cooled to room temperature and then reduced with pure hydrogen at 773 K for 1 h. The reaction feed consisted of: 0.3% NO + 0.2% ethanol in He. The reaction temperature varied between 493 and 593 K. The total flow rate was $250 \text{ cm}^3/\text{min}$ and the sample weight was 140 mg.

Table 1
BET and H_2/CO chemisorption results

Catalyst	Specific area (m^2/g)	Chemisorption	
		H_2 ($\mu\text{mol}/\text{g}_{\text{cat}}$)	CO ($\mu\text{mol}/\text{g}_{\text{cat}}$)
Pd-8Mo/ Al_2O_3	185	1.4	47
Pd/ $\text{Ce}_{0.75}\text{Zr}_{0.25}\text{O}_2$	85	27	76

3. Results and discussion

3.1. XRD, BET and CO and H_2 chemisorption

Fig. 1 shows the X-ray diffraction spectrum of the $\text{Ce}_{0.75}\text{Zr}_{0.25}\text{O}_2$ support used in this work. For comparison purposes, the spectra of a CeO_2 with cubic structure as well as a tetragonal and monoclinic phase mixture of ZrO_2 were shown.

It can be seen that the presence of zirconium shifted the CeO_2 lines at $2\theta = 28.6$ and 33.2° to $2\theta = 29.0$ and 33.6° . This has been attributed to the formation of a solid cerium–zirconium solution with a cubic structure [5].

Table 1 shows the BET and H_2/CO chemisorption results. The Pd-8Mo/ Al_2O_3 catalyst presented a higher specific area than the Pd/ $\text{Ce}_{0.75}\text{Zr}_{0.25}\text{O}_2$ catalyst. The hydrogen chemisorption results showed

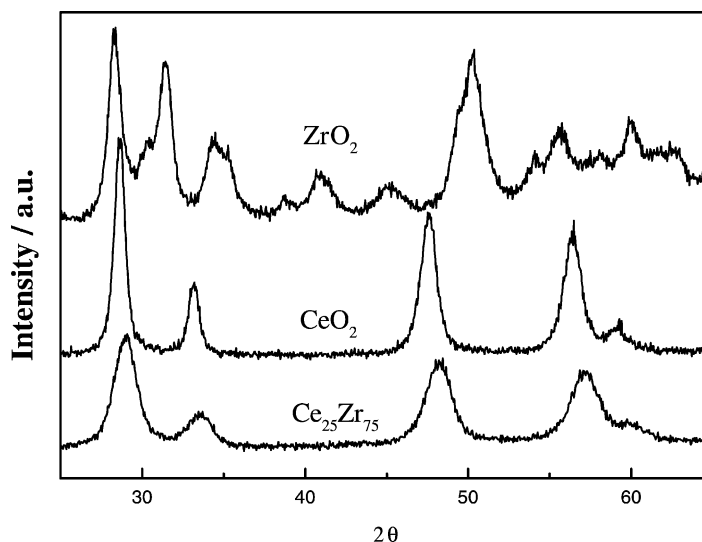


Fig. 1. X-ray diffraction spectrum results.

that the H_2 uptake was significantly higher for the Pd/Ce_{0.75}Zr_{0.25}O₂ catalyst when compared with the Pd-8Mo/Al₂O₃ catalyst. Previous results indicated that H_2 is not adsorbed on partially reduced molybdenum oxide and therefore, the value observed in Table 1 is due to chemisorption of H_2 on metallic sites [9].

For CO chemisorption it was observed, again, that the Pd/Ce_{0.75}Zr_{0.25}O₂ catalyst presented a higher value than the Pd-8Mo/Al₂O₃ catalyst. Furthermore, the amount of adsorbed CO was more than twice the amount of adsorbed hydrogen on both samples. More specifically, the amount of CO adsorbed on the Pd-8Mo sample was about 33 times higher than the amount of adsorbed H_2 , while on the Pd/Ce_{0.75}Zr_{0.25}O₂ this was almost 3 times. A possible explanation for this would be the adsorption of CO on the reduced oxides. In a previous work, IR measurements of adsorbed CO on Pd-8Mo/Al₂O₃ showed the presence of CO on partially reduced molybdenum oxide [8]. For the Pd/CeZrO₂ sample, another possibility (besides the adsorption of CO on the reduced support) would be the reduction of the mixed oxide by CO, with production of CO₂ and consequent formation of carbonates on the support. Indeed, the literature has been showing a great reducibility of the CeZrO₂ support and this has been attributed to the large mobility of the oxygen on the support due to the addition of ZrO₂ to the CeO₂ structure [3,11]. The addition of a noble metal promotes the reduction of this support at lower temperatures [12]. However, it is important to stress that catalysts were previously reduced at 500 °C/h, under pure hydrogen before chemisorption analysis and further reduction of the CeZrO₂ support (at room temperature) is unlikely. Therefore, it is possible that a rather small amount of adsorption of CO on partially reduced CeZrO₂ may have contributed to the excess amount of chemisorbed CO.

3.2. Temperature programmed desorption of adsorbed NO

Figs. 2 and 3 show the TPD profile after adsorption of NO on Pd-8Mo/Al₂O₃ and Pd/Ce_{0.75}Zr_{0.25}O₂ catalysts, respectively. Virtually no NO desorption was seen for the Pd-8Mo catalyst, while a great formation of N₂ (554 and 800 K) and a small formation of N₂O (405 and 537 K) were observed. According to the literature [13,14], the presence of a reducible oxide would

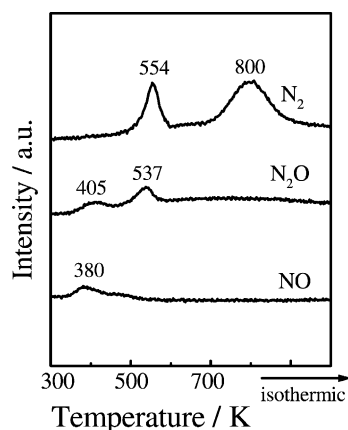


Fig. 2. TPD of adsorbed NO on Pd-8Mo/Al₂O₃ catalyst.

increase NO dissociation to N₂ and N₂O, suggesting that the reduced species of these oxides participate in this process. In previous works [8,9,13], the adsorption and dissociation of NO on partially reduced molybdenum oxide species was confirmed by TPD and IR measurements of adsorbed NO on Mo/Al₂O₃ and Pd-Mo/Al₂O₃ catalysts.

For the Pd/Ce_{0.75}Zr_{0.25}O₂, a significant dissociation of NO to N₂ and N₂O during adsorption at room temperature was observed (not shown). This fact was not detected for the Pd-8Mo/Al₂O₃ catalyst, which suggests that the Ce_{0.75}Zr_{0.25}O₂ mixed oxide has a greater NO dissociation ability than the partially reduced molybdenum oxide.

Comparing the TPD profiles of adsorbed NO on both samples (Figs. 2 and 3), it may be seen that the formation of N₂ and N₂O on Pd/Ce_{0.75}Zr_{0.25}O₂ occurred at a lower temperature range when compared to Pd-8Mo/Al₂O₃. Vesecky et al. [15] studied the CO + NO reaction on Pd/Al₂O₃ and on Pd(1 0 0) and Pd(1 1 1) surfaces. They observed that during NO decomposition, two adsorbed nitrogen species (N_a) are formed: thermally stable and less stable species. According to the authors, such species may be recombined to form N₂ at low temperatures (less stable species) and high temperatures (stable species). The authors also verified that the formation of stable N_a species hampers further NO adsorption and dissociation, thus affecting the reaction. They affirmed that smaller Pd particles favor NO dissociation to stable N_a species while larger particles tend to stabilize the adsorption of molecular NO.

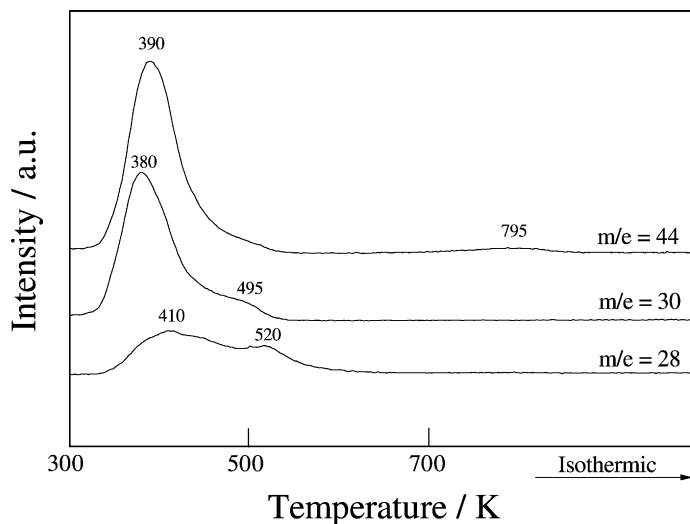


Fig. 3. TPD of adsorbed NO on Pd/Ce_{0.75}Zr_{0.25}O₂ catalyst.

Therefore, the Pd/Ce_{0.75}Zr_{0.25}O₂ catalyst seems to favor the formation of active nitrogen species (less stable N_a) whereas the Pd-8Mo/Al₂O₃ catalyst forms both less stable active species (low temperature N₂) as well as more stable active species (high temperature N₂).

3.3. Temperature programmed desorption of adsorbed ethanol

The TPD profile after adsorption of ethanol on Pd-8Mo/Al₂O₃ and Pd/Ce_{0.75}Zr_{0.25}O₂ are presented in Figs. 4 and 5, respectively. On both samples, ethanol desorption was observed around 400 K (reversibly adsorbed ethanol). The main difference between the catalysts was towards the decomposition products and the temperature of their formation. For the Pd/Ce_{0.75}Zr_{0.25}O₂ catalyst there was mainly formation of CO (695 K) and CO₂ (644 and 834 K) while on Pd-8Mo/Al₂O₃ there was considerable formation of ethylene (525 K) and acetaldehyde (478 and 525 K) besides the simultaneous formation of CO and CH₄ (480 K).

In a previous study [9], TPD analyses of adsorbed ethanol on Al₂O₃ and Pd/Al₂O₃ catalysts were made. For the support, a great formation of ethylene was observed and attributed to the dehydration of ethanol on the alumina acid sites. In the presence of Pd,

there was also the simultaneous formation of CO and CH₄ around 480 K and acetaldehyde was also seen at 478 K. Comparing these results with what was presented here for the Pd-8Mo catalyst (Fig. 4), it is clear that the formation of CO and CH₄ at 480 K is due to the direct decomposition of ethanol on Pd particles, while ethylene formation is characteristic of alumina. Cordi and Falconer [16] obtained a very similar result while studying adsorption properties of ethanol on Pd/Al₂O₃ catalysts. Since the exposed alumina surface was much higher than the Pd surface,

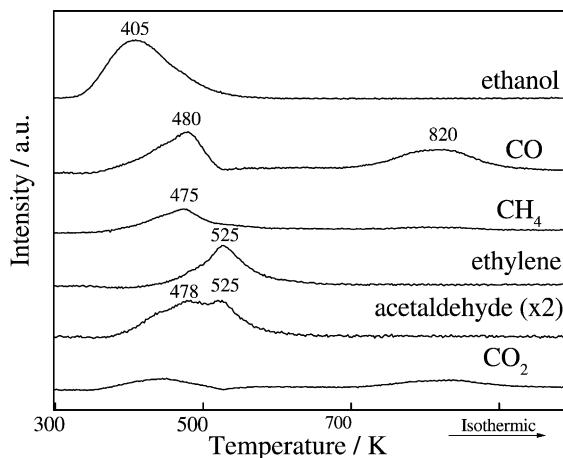


Fig. 4. TPD of adsorbed ethanol on Pd-8Mo/Al₂O₃ catalyst.

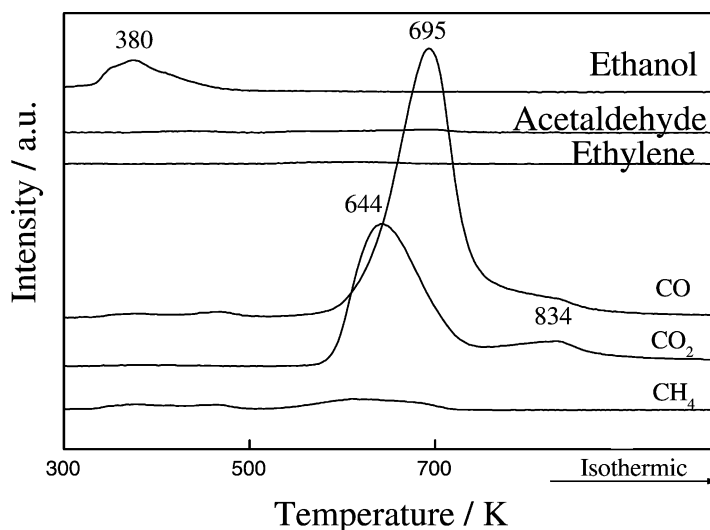


Fig. 5. TPD of adsorbed ethanol on Pd/Ce_{0.75}Zr_{0.25}O₂ catalyst.

the authors suggested that part of the ethanol adsorbed on alumina diffused to Pd sites to decompose. According to them, the α -carbon formed CO and the β -carbon formed CH₄ during ethanol decomposition. Furthermore, the formation of acetaldehyde at 478 K corresponds to the dehydrogenation of ethanol on Pd sites while the acetaldehyde peak at 525 K shown in Fig. 4 is probably related with the oxidative dehydrogenation of ethanol on partially reduced molybdenum oxide.

Another feature presented by the Pd-8Mo/Al₂O₃ catalyst was the production of CO and CO₂ at high temperatures (above 750 K). This was also observed for the Pd/Al₂O₃ catalyst studied previously [9]. IR measurements of adsorbed ethanol on Pd/Al₂O₃ showed that as decomposition took place (at lower temperatures), stable acetate species were formed and thus the high temperature CO and CO₂ formation during TPD was attributed to the decomposition of such species [9]. Therefore, for the Pd-8Mo/Al₂O₃ catalyst, the high temperature CO and CO₂ formation may be due to the decomposition of acetate species, which are formed during ethanol decomposition.

Since alumina is not present, no formation of ethylene was observed for the catalyst of Pd supported on CeZrO₂ mixed oxide (Fig. 5). Furthermore, neither acetaldehyde nor simultaneous formation of CO and CH₄ at low temperature were seen. As discussed

before, these products were mainly originated by the decomposition of ethanol, which was adsorbed on the alumina surface and diffused to Pd sites. This suggests that ethanol adsorbs more strongly on the mixed oxide surface and does not diffuse to palladium sites to decompose. Instead, it remains adsorbed until higher temperatures.

Unlike the partially reduced molybdenum oxide, the reduced mixed CeZr oxide did not promote oxidative dehydrogenation of ethanol (since no acetaldehyde was observed). On the other hand, large peaks of CO₂ and CO were seen at temperatures at least 150 K lower than the high temperature formation of CO and CO₂ on Pd-8Mo/Al₂O₃. Apparently, the Pd/Ce_{0.75}Zr_{0.25}O₂ catalyst favors total decomposition and/or oxidation of ethanol. In addition, an interesting fact is that the formation of CO₂ and CO was not simultaneous. There are two possible explanations for this and the first would be that as ethanol decomposes on the partially reduced mixed oxide, the decomposition products (CO and/or CH₄) would be oxidized to form CO₂. As the oxidation capacity diminishes, CO₂ formation decreases and CO (partial oxidation product) increases. The other possibility is that as the adsorbed ethanol is decomposed and/or oxidized, the CO formed would re-adsorb on the mixed oxide, desorbing only at higher temperature. This, however, is not yet very clear.

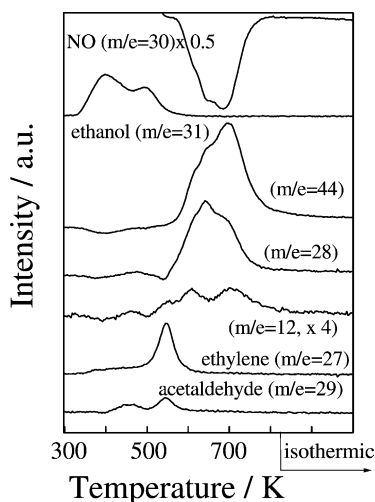


Fig. 6. TPSR on Pd-8Mo/Al₂O₃ catalyst.

3.4. Temperature programmed surface reaction

The TPSR profiles for the Pd-8Mo/Al₂O₃ and Pd/Ce_{0.75}Zr_{0.25}O₂ catalysts are displayed in Figs. 6 and 7, respectively. For the Pd-8Mo, ethanol desorption was observed at 400 and 490 K, ethylene was formed around 545 K and the simultaneous formation of CO, CH₄ and H₂ (previously observed during TPD) was not seen. A small amount of acetaldehyde was detected around 455 and 545 K. NO consumption began at higher temperatures, showing a well defined peak at 690 K and two small shoulders around 640

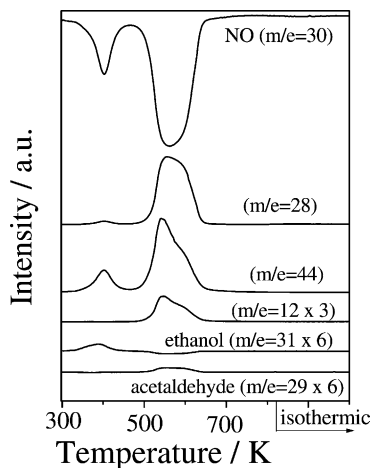


Fig. 7. TPSR on Pd/Ce_{0.75}Zr_{0.25}O₂ catalyst.

and 612 K. The NO consumption was followed by the simultaneous increase in the intensity of signals $m/e = 44$ and 28 (possibly associated with N₂O, CO₂, N₂ or CO). On the other hand, the signal $m/e = 12$ (associated with CO and/or CO₂ formation) was seen only around 605 and 695 K.

Comparing the TPSR profile with the TPD of adsorbed ethanol (Fig. 4), it may be seen that instead of the simultaneous formation of CO and CH₄ around 480 K, there was desorption of ethanol at 490 K. As discussed above, the formation of CO and CH₄ is due to decomposition of ethanol on Pd sites. Therefore, this indicates that in the presence of NO, ethanol does not decompose on Pd, thus suggesting that NO adsorbs preferentially on Pd, not allowing ethanol decomposition to take place. Acetaldehyde formation was similar and is probably due to the oxidative dehydrogenation of ethanol on partially reduced molybdenum oxide.

An interesting fact is that NO consumption peaks were observed only above 600 K, after ethanol was desorbed or dehydrogenated. However, the TPD analysis of adsorbed NO (Fig. 2) showed that for the Pd-8Mo catalyst, NO decomposition took place below 550 K (N₂ and N₂O formation). The above results suggest that ethanol competes with NO for adsorption sites on MoO_x species and NO adsorption occurs only after ethanol desorbs. As mentioned before, NO consumption was followed by the increase in the intensity of signals $m/e = 44$ and 28. This may be due to either NO decomposition (with formation of N₂ and N₂O) or reaction of NO with acetate species (same acetate species responsible for CO and CO₂ formation at high temperature during TPD of adsorbed ethanol). In this case, the reaction products could be N₂, N₂O, CO or CO₂. In fact, the signal $m/e = 12$, which is a secondary mass fragment of CO and/or CO₂ was seen at 605 and 695 K. This indicates that reaction between NO and acetate species does take place, although simultaneous NO decomposition may not be ruled out (and is also most likely to happen).

The TPSR profile for the Pd/Ce_{0.75}Zr_{0.25}O₂ catalyst (Fig. 7) showed NO consumption in two distinct peaks (400 and 560 K). The first peak was followed by an increase in the intensity of the signal $m/e = 44$ (probably N₂O formation) and also a very small increase in the intensity of $m/e = 28$ (N₂ formation). The second consumption peak was followed by increases in the intensity of the signals $m/e = 44$, 28 and 12. Ethanol

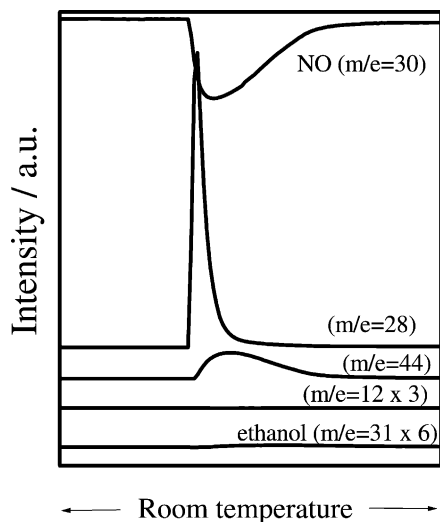


Fig. 8. Room temperature NO flow prior to TPSR on Pd/Ce_{0.75}Zr_{0.25}O₂ catalyst.

desorption was seen at 385 K and a small formation of acetaldehyde was observed around 560 K. For this sample, it is worth mentioning that, as NO flow was let into the reactor, at room temperature (after ethanol adsorption was finished), there was a very large peak of signals $m/e = 28$ and 44 without the simultaneous increase in signal $m/e = 12$ or ethanol desorption (Fig. 8). This indicates that NO decomposition with formation of N₂ and N₂O occurred at room temperature in agreement with TPD measurements and was not influenced by the presence of adsorbed ethanol.

Unlike the Pd-8Mo catalyst, on Pd/Ce_{0.75}Zr_{0.25}O₂ it was not necessary for ethanol decomposition or desorption to take place for NO adsorption and decomposition to happen. This suggests that there are different adsorption sites for NO and ethanol on the mixed oxide surface. This was confirmed as the temperature was raised and NO consumption occurred in the same temperature range as NO decomposition during TPD (Fig. 3). Reaction between NO and adsorbed carbon species began around 520 K until 630 K. In fact, in this temperature range, there was an increase in the intensity of the signal $m/e = 12$, indicating formation of CO/CO₂.

During TPD of adsorbed ethanol (Fig. 5), CO and CO₂ were detected only above 600 K, which confirms that the formation of such products during TPSR is probably due to the reaction of NO with adsorbed car-

bon species. It is important to notice that this reaction occurred at lower temperatures than on the Pd-8Mo catalyst (Fig. 6), indicating that the Pd/Ce_{0.75}Zr_{0.25}O₂ is more active for this reaction. Furthermore, acetaldehyde (partial oxidation product) was detected around 560 K and this was not due to dehydrogenation of adsorbed ethanol, since during TPD (Fig. 5) acetaldehyde was not observed at all. Hence, acetaldehyde was formed as a product originated from the reaction of NO with adsorbed carbon species.

3.5. Catalytic test

The results for NO and ethanol conversion and also the selectivity values for N₂ and carbon species formation are presented in Fig. 9 and Table 2, respectively. It may be seen in Fig. 9 that for the Pd-8Mo catalyst the NO conversion was higher than ethanol conversion. However, the selectivity values for carbon species, presented in Table 2, show some formation of ethylene, which is a product from the dehydration of ethanol on alumina, as discussed above, suggesting, there is a parallel reaction of ethanol consumption occurring on the alumina surface. For this catalyst, the selectivity values for the formation of N₂ (Table 2) were constant. In a prior study [9], the NO + ethanol reaction was carried out in a Pd/Al₂O₃ catalyst and it was verified that, not only the selectivity for N₂ formation was constant, but it was also the same as presented here for the Pd-8Mo catalyst. This suggests that the N₂ production mechanism is the same on both catalysts, regardless of the presence of the molybdenum oxide. It seems that for the NO + ethanol reaction, the addition of MoO₃ on Pd/Al₂O₃ does not have a promoting effect, as was observed before for the NO + CO reaction [8]. Apparently, there is a different mechanism than the redox mechanism proposed for the reduction of NO with CO on Pd-Mo catalysts, where NO adsorbs and dissociates on the partially reduced molybdenum oxide and the oxygen from the NO molecule is used for the oxidation of CO on the Pd sites. In fact, the TPSR results showed that NO adsorbs preferentially on Pd sites, not allowing ethanol adsorption, whereas ethanol competes with NO for adsorption sites on the partially reduced molybdenum oxide. Therefore, the reaction pathway for the NO + ethanol reaction should be different than the redox mechanism mentioned before.

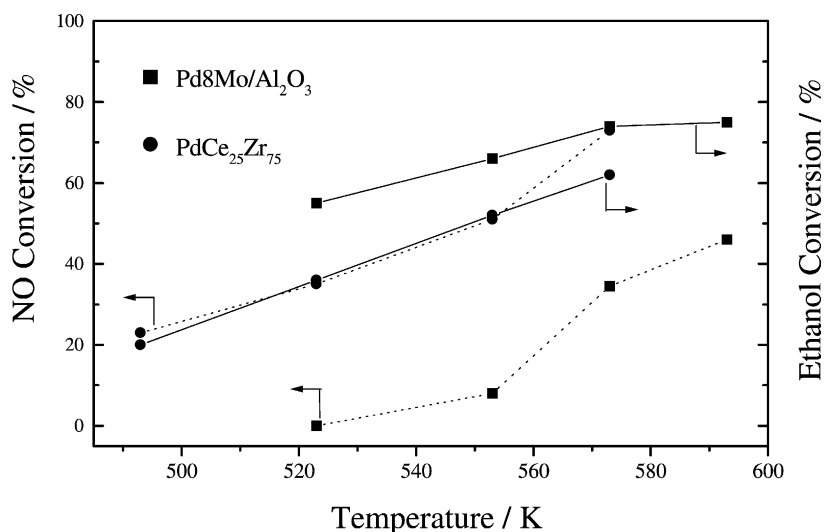


Fig. 9. NO and ethanol conversion vs. temperature.

The Pd/CeZrO₂ catalyst was more active for the NO reduction with ethanol, showing higher NO conversion levels when compared to the Pd-8Mo catalyst (Fig. 9). Unlike the Pd-8Mo sample, N₂ selectivity increased as the temperature was raised (Table 2). The selectivity for carbon species was also different than that observed for the Pd-8Mo catalyst. There was little formation of acetaldehyde (also observed during TPSR) and CO₂ (total oxidation product) was the main carbon-containing specie formed. These results suggest that, although both samples contain reducible oxides, there are distinct mechanisms for the reduction of NO with ethanol. The TPD of adsorbed NO showed

that the CeZr mixed oxide is more reducible and has a higher NO dissociation capacity than the molybdenum oxide. Besides that, the TPD of adsorbed ethanol showed that on Pd/Ce_{0.75}Zr_{0.25}O₂ there was higher CO₂ formation from decomposition/oxidation of adsorbed ethanol, and also that ethanol does not diffuse to Pd sites to decompose. Furthermore, the TPSR results indicated that, unlike the Pd-8Mo sample, NO does not compete for adsorption sites with ethanol on the mixed oxide surface.

These results lead us to believe that it is possible that the decomposition and/or dissociation reactions of both NO and ethanol on the Ce_{0.75}Zr_{0.25}O₂ support

Table 2
Selectivity values for the reduction of NO with ethanol

Catalyst	Temperature (K)	N ₂ selectivity ^a (%)	Selectivity for carbon species (%)			
			CO	CO ₂	Acetaldehyde	Ethylene
Pd-8Mo/Al ₂ O ₃	523	–	30	61	0	9
	553	61	44	50	0	6
	573	67	38	47	0	15
	593	68	34.5	40.5	0	25
Pd/Ce _{0.75} Zr _{0.25} O ₂	493	35	6	87	7	0
	523	69	6	84	11	0
	553	83	4	91	5	0
	573	86	5	87	8	0

^a N₂ selectivity calculated considering N₂ and N₂O formation.

play an important role in the reaction mechanism for this catalyst. Such side reactions might contribute to the higher activity and N_2 and CO_2 selectivity presented by the $\text{Pd/Ce}_{0.75}\text{Zr}_{0.25}\text{O}_2$ catalyst. Apparently, the fact that $\text{Ce}_{0.75}\text{Zr}_{0.25}\text{O}_2$ is more reducible than MoO_3 considerably affects the $\text{NO} + \text{ethanol}$ reaction.

4. Conclusion

The $\text{Pd/CeO}_2\text{-ZrO}_2$ catalyst was more active for NO conversion and also showed higher selectivity for N_2 and CO_2 formation when compared with the $\text{Pd-MoO}_3/\text{Al}_2\text{O}_3$ catalyst. TPD analyses of adsorbed NO and ethanol revealed that Ce-Zr has a higher ability to dissociate NO to N_2 , and also to decompose ethanol with formation of CO_2 . Furthermore, the TPSR experiments showed that on Pd-8Mo , NO adsorbs preferentially on Pd sites and ethanol competes with NO for adsorption sites on partially reduced molybdenum oxide. This was not the case for the $\text{Ce}_{0.75}\text{Zr}_{0.25}\text{O}_2$ catalyst, where both NO and ethanol adsorb and decompose on the partially reduced mixed oxide surface. The TPSR results also revealed that the reaction between NO and adsorbed carbon species takes place with formation of N_2 , N_2O , CO and CO_2 . For this reaction, the $\text{Pd/Ce}_{0.75}\text{Zr}_{0.25}\text{O}_2$ was more active, agreeing well with the results from the catalytic tests. Apparently, these differences considerably affect the $\text{NO} + \text{ethanol}$ reaction and are related with the

better performance of the $\text{Pd/Ce}_{0.75}\text{Zr}_{0.25}\text{O}_2$ catalyst when compared to the $\text{Pd-MoO}_3/\text{Al}_2\text{O}_3$ catalyst.

References

- [1] R.M. Heck, R.J. Farrauto, *Catalytic Air Pollution Control: Commercial Technology*, Van Nostrand Reinhold, New York, 1995, p. 147.
- [2] K. Taylor, *Catal. Rev.* 35 (1993) 457.
- [3] P. Fornasiero, J. Kaspar, V. Sergo, M. Graziani, *J. Catal.* 182 (1999) 56.
- [4] J. Kaspar, P. Fornasiero, M. Graziani, *Catal. Today* 50 (1999) 285.
- [5] C.E. Hori, H. Permana, K.Y. Simon Ng, A. Brenner, K. More, K.M. Rahmoeller, D. Belton, *Appl. Catal. B: Environ.* 16 (1998) 105.
- [6] P. Fornasiero, G. Ranga Rao, J. Kaspar, F. L'Erario, M. Graziani, *J. Catal.* 175 (1998) 269.
- [7] R. Di Monte, P. Fornasiero, J. Kaspar, P. Rumori, G. Gubitosa, M. Graziani, *Appl. Catal. B: Environ.* 24 (2000) 157.
- [8] M. Schmal, M.A.S. Baldanza, M.A. Vannice, *J. Catal.* 185 (1999) 138.
- [9] M.A.S. Baldanza, L.F. de Mello, M.A. Vannice, F.B. Noronha, M. Schmal, *J. Catal.* 192 (2000) 64.
- [10] J.E. Benson, H.S. Hwang, M. Boudart, *J. Catal.* 30 (1973) 46.
- [11] J. Kaspar, P. Fornasiero, M. Graziani, *Catal. Today* 285 (1999) 50.
- [12] P. Fornasiero, R. Di Monte, G. Rao Rao, J. Kaspar, S. Meriani, A. Trovarelli, M. Graziani, *J. Catal.* 151 (1995) 168.
- [13] M.A.S. Baldanza, F.B. Noronha, M. Schmal, *J. Catal.* 188 (1999) 270.
- [14] H. Cordatos, R.J. Gorte, *J. Catal.* 159 (1996) 112.
- [15] S.M. Vesecky, D.R. Rainer, D.W. Goodman, *J. Vac. Sci. Technol.* 14 (1996) 1457.
- [16] E.M. Cordi, J.L. Falconer, *J. Catal.* 162 (1996) 104.